Freehand millimeter-wave imaging system based on a highly-integrated MIMO radar module

Guillermo Álvarez-Narciandi[a,b], Jaime Laviada[a], and Fernando Las-Heras[a]

[a]Group of Signal Theory and Communications, University of Oviedo, 33203 Gijón, Spain
[b]Centre for Wireless Innovation, Queen's University Belfast, BT39DT Belfast, United Kingdom

ABSTRACT

In this contribution, a portable freehand millimeter-wave imaging system based on a highly integrated radar-on-chip module is presented. The small imager can be easily moved by hand to scan local suspicious areas. The freehand movement of the imager is tracked by an optical system enabling to apply synthetic aperture radar processing techniques, yielding enhanced lateral resolution compared to standalone acquisitions. The commercial radar module comprises up to 400 independent radiofrequency channels, allowing the retrieval of high-resolution images at a fast scanning rate. Furthermore, the imaging system significantly outperforms other compact imagers based on radiofrequency front-ends with a lower degree of integration of transmitters and receivers (i.e., with less radiofrequency channels) in terms of image quality, as the impact of positioning errors is mitigated. The performance and scanning capabilities of the proposed freehand imaging system are illustrated through measurements of different test targets. This system provides a fair trade-off between flexibility, scanning speed, and cost-effectiveness of the imager, making it very convenient for situations in which the usage of large scanners is not practical nor affordable. In addition, this imaging approach paves to way to the integration of millimeter-wave electromagnetic imaging scanning capabilities in general purpose devices, enabling the use of this sensing modality in a wide-range of applications.

Keywords: Freehand imaging, radar, mmWave imaging, MIMO, real-time system, optical tracking system

1. INTRODUCTION

Electromagnetic imaging enables the reconstruction of images from electromagnetic signals, which are capable of penetrating certain materials which are opaque at visible wavelengths.[1] This is of significant interest for a wide number of applications such as security screening,[2,3] landmine detection,[4] medical diagnosis[5,6] or non-destructive evaluation[7] to name a few. Although imaging systems rely on different architectures and implementations, one of the most popular imaging approaches is based on synthetic aperture radar (SAR), in which the lateral resolution depends on the size of the synthesized aperture. These systems can be implemented resorting to a significant number of transmitters (TXs) and receivers (RXs) to create a large aperture,[2] performing a raster scan of a small set of TXs and RXs, or using a reduced number of TXs and RXs in a MIMO configuration.[8] These systems are able to produce high-resolution images, but they either have a considerable size, or require the use of heavy positioning equipment, which may prevent their use for certain applications. A trade-off between resolution and compactness has been achieved with the microwave cameras presented in Ref. 7 and Ref. 9, respectively. Both of them employ medium-sized apertures in the range $[20, 30]$ cm, which makes them portable, though slightly bulky. This entails a resolution loss, which is partially compensated by a shorting scanning distance. A different approach referred to as freehand imaging was presented in Ref. 10, 11. The main goal of this imaging modality, which takes advantage of the latest developments of millimeter-wave (mmWave) technology and tracking systems, is to enable the use of handheld imagers, overcoming movement constraints and thus increasing its flexibility, to produce high-resolution images. For that purpose, it is necessary to resort to compact radiofrequency front-ends, such as a radar-on-chip module,[12] which can be embedded in a general purpose device such a smartphone.[13] In addition, as the physical aperture of these compact radiofrequency front-ends is too small to obtain high-resolution images, a tracking system must be used to generate a synthetic aperture. Therefore, the operator

Further author information: (Send correspondence to G.A.N.)
G.A.N.: E-mail: alvareznguillermo@uniovi.es

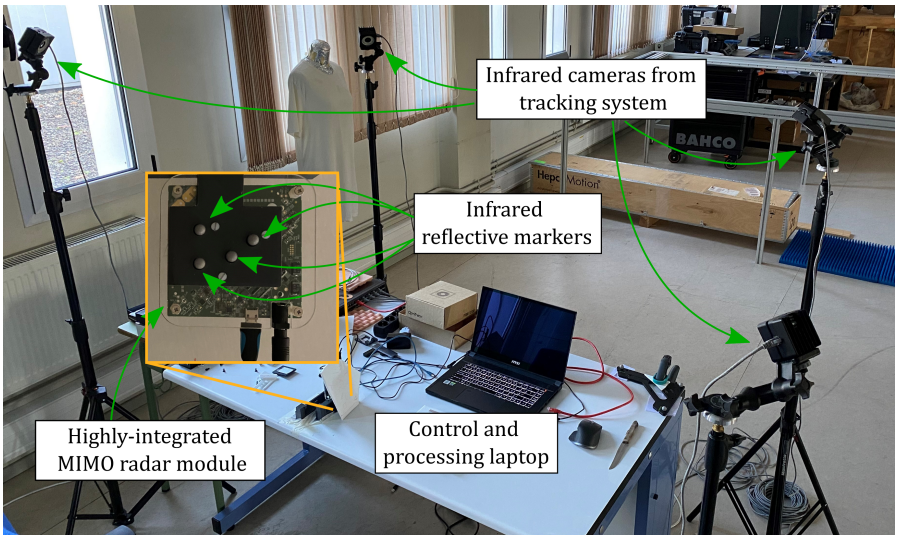

Figure 1. Measurement setup including the infrared cameras of the optical tracking system, the control and processing laptop, and the highly-integrated MIMO radar module. A detailed picture of the radar module is shown in the inset.

of the handheld imager moves by hand the radiofrequency front-end over the area under inspection while its position is tracked. Moreover, real-time results can be displayed to the operator to dinamically decide where to continue the scan. Some of the challenges faced by freehand imagers are that they require processing algorithms capable of dealing with non-uniformly acquired samples due to the freehand movement of the scanner, and that are also capable of providing real-time updates of the results.[14] This contribution presents a freehand imager that leverages a highly integrated radar-on-chip module commercialized by Vayyar. It comprises 50 times the amount of independent TX-RX pairs (i.e., independent radiofrequency channels) of the radar on chip employed in the freehand systems presented in Ref. 10, 11, while keeping a reduced size. As a consequence, the scanning speed is increased and higher quality images can be achieved, as positioning errors are mitigated.

2. SYSTEM DESCRIPTION

The presented system uses a mmWave frequency-stepped continues-wave radar-on-chip module designed by Vayyar,[15] which comprises 20 TXs and 20 RXs. The transmitters are sequencially activated, while the receivers operate concurrently, yielding a total of 400 independent radiofrequency channels. The frequency ranges from 62 GHz to 69 GHz, and the time required for a complete acquisition of all the radiofrequency channels is 200 ms. The radar module is tracked by means of an optical tracking system[16] formed by four infrared cameras, and four reflective markers attached to the radar module, which provide submillimeter accuracy. The cameras are deployed around the area of interest and can be easily calibrated in a few minutes. Figure 1 depicts the measurement setup including the radar module, the tracking system, and the control laptop. This laptop triggers the radar and position acquisitions, and process the acquired data in real-time displaying the updated results to the operator.

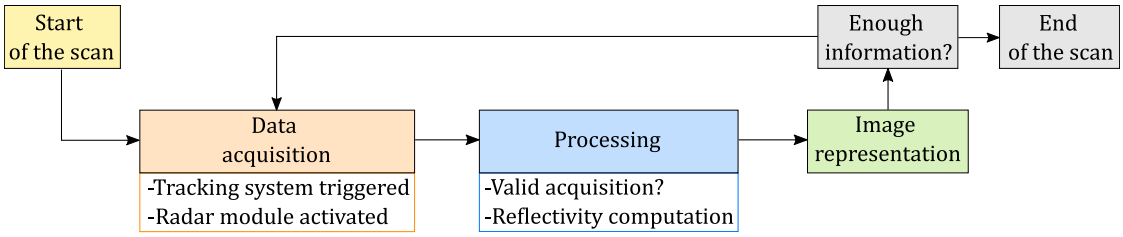

Figure 2. Processing workflow of the presented system.

The workflow of the system is summarized in Figure 2. As it can be seen, the reflectivity of the investigation domain is updated after each acquisition as the operator moves the scanner over the area of interest. In particular, after the m-th acquisition is performed at the position of the radar module $\mathbf{r}$, the reflectivity, ρ, of the points of the investigation domain, $\mathbf{r}'$, is updated using a delay-and-sum algorithm:

$$\rho_m(\mathbf{r}') = \sum_{i=1}^{m} \sum_{p=1}^{N_{RX}} \sum_{n=1}^{N_{TX}} S_{i,p,n}(\mathbf{r}, f) e^{\frac{2\pi f}{c}(||\mathbf{r}'-\mathbf{r_{tx,n}}||+||\mathbf{r}'-\mathbf{r_{rx,p}}||)}, \tag{1}$$

where f denotes the frequency, c the speed of light, and the position of the n-th transmitter and that of the p-th receiver of the radar module at the m-th acquisition are $\mathbf{r_{tx,n}}$ and $\mathbf{r_{rx,p}}$, respectively.

It should be noted that, in order to ensure an adequate sampling, avoiding oversampled areas, the area over the investigation domain where the operator moves the imager is discretized in cells of size $\lambda/2 \times \lambda/2 \times \lambda/2$. Within each of these cells only N_{max} acquisitions are allowed and after that number is reached posterior acquisitions are discarded.[10] After the reflectivity has been computed, the results are displayed to the operator, who can decide if enough information has been acquired, or if further acquisitions are required.

3. RESULTS

In order to test the performance of the system, the pocket knife depicted in Figure 3(a) was scanned. During the measurement a total of 1056 samples were acquired. The distribution of these samples can be observed in Figure 3(d). In this case, the maximum number of acquisitions per cell was set to $N_{max} = 1$. An intermediate result obtained after 300 acquisitions were performed, approximately a third of all the measurements, is shown in Figure 3(b). As it can be seen, this image is sufficient to identify the pocket knife, although there is more clutter than in the image obtained at the end of the scan. This image is depicted in Figure 3(c), where it can be observed the reduced level of clutter. In addition, the shape of the blade, and the details of the handle can be distinguished. Depending on the kind of application in which the imager is used, it may only be necessary to identify a potentially dangerous object or an anomaly within the area under inspection, or it may be required a higher level of details, in which case a longer and more thorough scan is required. The presented system enables this flexibility, providing its operator the ability to decide on-the-fly if more measurements are required. Moreover, the high number of independent transmitter-receiver channels of the radar module contributes to increase the scanning speed, while positioning errors are mitigated.

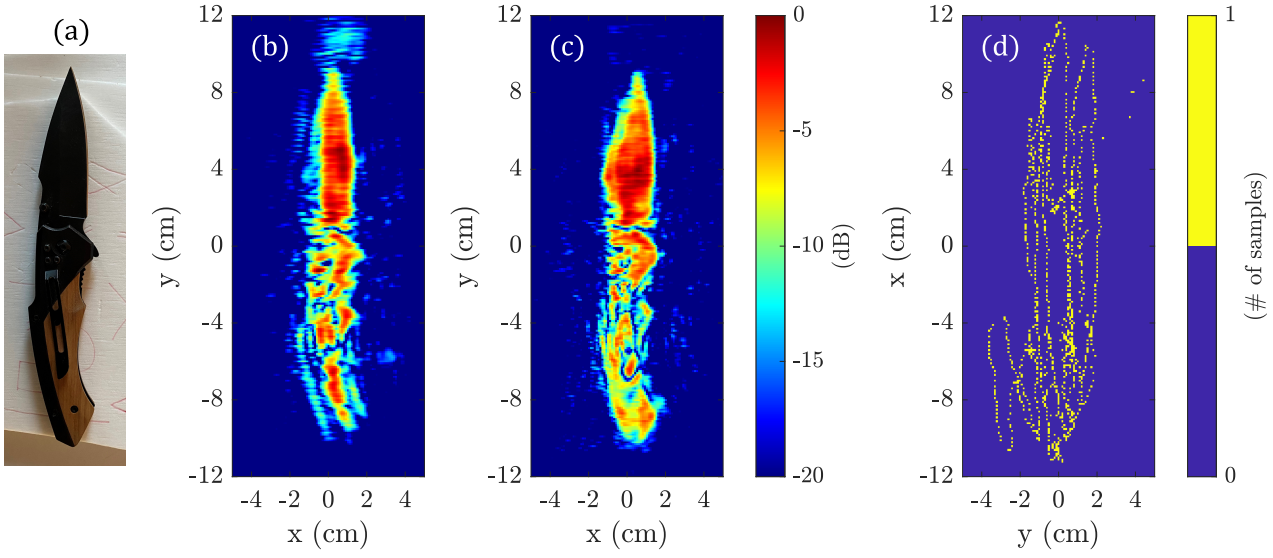

Figure 3. (a) Image of the pocket knife used as test target, reflectivity image of the target (b) after 300 acquisitions, and (c) after the whole scan, and (d) distribution of the acquisitions performed during the scan.

4. CONCLUSIONS

This contribution presents a freehand imaging system based on a commercialy available highly-integrated MIMO radar module comprising 400 independent transmitter-receiver channels. The position and orientation of this module is estimated by means of an optical tracking system based on the use of infrared cameras and reflective markers with submillimeter accuracy. As a result, the operator of the system can move the radar module over the area under inspection acquiring measurements, which can be coherently combined. Thus, high-resolution images can be obtained with a compact handheld device, conferring great flexibility to the system and paving the way to the adoption of mmWave imaging in applications where the use of large scanners is not feasible. Results show that only a few samples are required to generate an electromagnetic image sufficiently accurate to identify the shape of a complex target, in this case a pocket knife. Moreover, if a longer scan is performed, even small details of the target can be retrieved.

ACKNOWLEDGMENTS

This work has been funded by the Ministerio de Ciencia, Innovación y Universidades of Spain /FEDER under project RTI2018-095825-B-I00 ("Millihand") and project PID2021-122697OB-I00; by the Ministry of Universities of Spain and European Union - NextGenerationEU - under grant MU-21-UP2021-030-71667225; and by Gobierno del Principado de Asturias/FEDER under grant AYUD/2021/51706.

REFERENCES

[1] Pastorino, M., [*Microwave Imaging*], John Wiley & Sons, Inc. (2010).

[2] Sheen, D. M., McMakin, D. L., and Hall, T. E., "Three-dimensional millimeter-wave imaging for concealed weapon detection," *IEEE Trans. Microw. Theory Techn.* **49**, 1581–1592 (Sep 2001).

[3] Gollub, J. and et al., "Large metasurface aperture for millimeter wave computational imaging at the human-scale," *Sci Rep* **7**(42650) (2017).

[4] Garcia-Fernandez, M., Alvarez-Lopez, Y., and Las Heras, F., "Autonomous Airborne 3D SAR Imaging System for Subsurface Sensing: UWB-GPR on Board a UAV for Landmine and IED Detection," *Remote Sensing* **11**(20) (2019).

[5] Klemm, M., Craddock, I. J., Leendertz, J. A., Preece, A., and Benjamin, R., "Improved delay-and-sum beamforming algorithm for breast cancer detection," *International Journal of Antennas and Propagation* (2008).

[6] Bevacqua, M. T., Di Meo, S., Crocco, L., Isernia, T., and Pasian, M., "Millimeter-waves breast cancer imaging via inverse scattering techniques," *IEEE Journal of Electromagnetics, RF and Microwaves in Medicine and Biology* **5**(3), 246–253 (2021).

[7] Ghasr, M. T., Horst, M. J., Dvorsky, M. R., and Zoughi, R., "Wideband microwave camera for real-time 3-d imaging," *IEEE Trans. Antennas Propag.* **65**, 258 – 268 (Jan 2017).

[8] Ahmed, S. S., Schiessl, A., and Schmidt, L. P., "A novel fully electronic active real-time imager based on a planar multistatic sparse array," *IEEE Trans. Microw. Theory Techn.* **59**, 3567–3576 (Dec 2011).

[9] Hussung, R., Keil, A., and Friederich, F., "Handheld millimeter wave imaging system based on a two-dimensional multistatic sparse array," in [*2020 45th International Conference on Infrared, Millimeter, and Terahertz Waves (IRMMW-THz)*], 1–2 (2020).

[10] Álvarez Narciandi, G., López-Portugués, M., Las-Heras, F., and Laviada, J., "Freehand, agile, and high-resolution imaging with compact mm-wave radar," *IEEE Access* **7**, 95516–95526 (2019).

[11] Álvarez Narciandi, G., Laviada, J., and Las-Heras, F., "Freehand mm-wave imaging with a compact mimo radar," *IEEE Transactions on Antennas and Propagation* **69**(2), 1224–1229 (2021).

[12] Nasr, I., Jungmaier, R., Baheti, A., Noppeney, D., Bal, J. S., Wojnowski, M., Karagozler, E., Raja, H., Lien, J., Poupyrev, I., and Trotta, S., "A highly integrated 60 GHz 6-channel transceiver with antenna in package for smart sensing and short-range communications," *IEEE J. Solid-State Circuits* **51**, 2066–2076 (Sept 2016).

[13] Álvarez Narciandi, G., Laviada, J., and Las-Heras, F., "Towards turning smartphones into mmWave scanners," *IEEE Access* **9**, 45147–45154 (2021).

[14] Smith, J. W. and Torlak, M., "Efficient 3-D Near-Field MIMO-SAR Imaging for Irregular Scanning Geometries," *IEEE Access* **10**, 10283–10294 (2022).
[15] Vayyar, "System on chip specification," (Oct. 2021).
[16] OptiTrack, "Optitrack motion capture system," (Feb. 2022).